Intrinsic electronic structure of threading dislocations in GaN

I. Arslan and N. D. Browning
Department of Physics (M/C 273), University of Illinois at Chicago, 845 West Taylor Street, Chicago, Illinois 60607-7059
(Received 17 August 2001; published 25 January 2002)

In this paper we use multiple-scattering simulations in conjunction with experimental *Z*-contrast images and electron-energy-loss spectra to obtain a detailed analysis of the effect of the intrinsic structure of edge, screw, and mixed dislocations on the local density of unoccupied states in GaN. In particular, we show that the multiple scattering method is especially useful for examining dislocation cores where the bonding is significantly different at each atomic site in the structure. Furthermore, the analysis of the nitrogen *K* edge from intrinsic dislocations in GaN, i.e., stoichiometric cores with no dopants or vacancies, shows that the changes in the local electronic structure can be attributed to a change in the symmetry of the structure that does not result in readily identifiable states in the band gap. As such, the electrical activity at dislocations that limits the lifetime and performance of GaN devices appears to be related to the segregation of dopants, impurities or vacancies.

DOI: 10.1103/PhysRevB.65.075310 PACS number(s): 73.20.−r, 79.20.Uv, 61.10.Ht, 61.72.Ff

I. INTRODUCTION

Dislocations are known to exhibit a wide variety of effects that can have a significant impact on the mechanical, electrical, and optical properties of many materials.[1,2] One family of materials in which the properties of dislocations are particularly intriguing is gallium nitride (GaN) and its alloys.[3,4] High-performance light-emitting diodes (LED's) and lasers[5–7] have been fabricated using GaN despite a density of dislocations that is high enough to destroy such properties in other III-V materials.[8] However, while these devices function, their lifetime and efficiency are limited by the presence of these dislocations. It is not immediately clear how dislocations can have both a benign and detrimental effect, and this has led to an intensive research effort to understand their properties for both practical applications and from a basic materials science standpoint.

As a result of this widespread effort, there have been many conflicting views on the role of the threading dislocations in GaN, which to a great extent appears to depend on the fabrication method, doping level, and the history of the sample. For example, several cathodoluminescence experiments showed that dislocations are responsible for yellow luminescence,[9,10] indicating localized states in the band gap. However, Dassonneville *et al.*[11] asserted that while dislocations act as nonradiative recombination centers, they are not responsible for the yellow band. Furthermore, photoluminescence studies by Izumi *et al.*[12] indicated that threading dislocations do not limit the efficiency of devices significantly, and that the devices are in fact failing due to other, different types of nonradiative recombination centers in the material. Other experiments currently being conducted, including photoelectrochemical etching,[13] transport studies and modeling,[14,15] and scanning capacitance microscopy[16,17] have similar apparent contradictions in their findings. There are also notable inconsistencies in the theoretical simulations from dislocation cores in GaN. *Ab initio* calculations by Elsner and co-workers did not predict states in the band gap,[18,19] while similar calculations by Wright *et al.* concluded that under the majority of growth conditions, states in the band gap should be formed.[20] However, the majority of discrepancies in the predicted properties, both structurally and electronically, are due to the difficulty in distinguishing the intrinsic properties of the dislocation core from the effects of impurities and point defects.[21]

In an attempt to avoid some of the confusion surrounding dislocations in GaN, here we use multiple-scattering simulations[22–25] to investigate the intrinsic electronic structure of edge, screw, and mixed dislocations. By addressing the intrinsic structure, i.e., using stoichiometric cores with no segregated dopants, impurities, or vacancies, our aim is to understand how the creation of a dislocation core changes the local electronic structure. While intrinsic cores may be a rarity in real device materials, an analysis of the underlying core structure is an essential first step in developing a full understanding of how dislocation cores do or do not affect the overall device properties.

The structures of the cores used in this analysis (and therefore the clusters used for the multiple-scattering simulations) are obtained from a variety of methods, including experimental atomic resolution *Z*-contrast images,[26] *ab initio* calculations,[18,19] and a combination of linear elasticity[2] and bond-valence[27–30] analysis. The *Z*-contrast technique provides a direct image[31,32] of the atomic structure and composition of the cores, and allows a verification of the theoretical structures to be obtained. Furthermore, as the contrast is sensitive to the composition of the sample, the structures are known to contain at most ~10% impurities or vacancies, i.e., they are intrinsic structures.

Having defined the structures of the intrinsic dislocation cores, self-consistent multiple scattering simulations using the FEFF8 codes[22] are performed for the bulk and all three dislocations: an edge (*a* type) dislocation, a screw (*c* type) dislocation, and a mixed ($a+c$ type) dislocation. The resulting spectra were verified by comparison with experimental atomic resolution electron-energy-loss spectra[33,34] (EELS) from GaN dislocations with an edge component (*a* or $a+c$ type). The simulations of the nitrogen *K*-edge spectra revealed that there are distinctive changes in the electronic structure for each core, related to the structural distortions

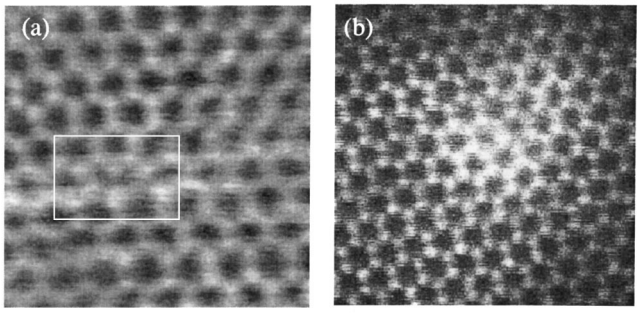

FIG. 1. *Z*-contrast images of a dislocation with (a) an edge component to its Burgers vector (a) and a screw dislocation (b). The edge component dislocation has an eight-atom ring structure, producing distortions in the *ab* plane. The screw dislocation has the hexagonal bulk symmetry in the *ab* plane, and distortions in the *c* direction, seen from the surrounding strain field (Ref. 33).

occurring within the *ab* plane and/or along the *c* axis. Furthermore, consistent with the experimental spectra, no obvious localized states are found in the band gap for any of the intrinsic core structures. These results indicate that, consistent with defect systems in oxides,[35] the observed effects at dislocations are most likely related to extrinsic effects, such as the segregation of vacancies, impurities, and dopants.

II. EXPERIMENTAL OBSERVATIONS FROM DISLOCATIONS IN GaN

The multiple-scattering simulations shown here are based on experimental results acquired on two scanning transmission electron microscopes (STEM).[34] The *Z*-contrast images shown in Fig. 1 were acquired from a VG HB603 dedicated STEM (Ref. 36) (an accelerating potential of 300 kV and a probe size ~0.13 nm), and the (EELS) shown in Fig. 2 were acquired from a JEOL 2010-F STEM (Ref. 37) (an accelerating potential of 200 kV and a probe size of ~0.13 nm). *Z*-contrast images are formed in the STEM by collecting the transmitted high-angle scattering on an annular detector as the electron probe is scanned over the surface of the specimen.[31] This high-angle, or Rutherford scattering, is approximately proportional to the square of the atomic number (hence the name *Z*-contrast imaging). The key advantage in the *Z*-contrast image for the analysis performed here is that coherent effects between the neighboring atomic columns are effectively averaged out, resulting in an incoherent (or direct) image of the structure.[31,32] The atomic columns in the core can therefore be identified directly from the image. Furthermore, the intensity in the columns is proportional to the composition, allowing the presence of impurities and vacancies to be detected.

The images in Fig. 1 show two of the three types of dislocations in thin-film GaN: an edge (or a dislocation with an edge component) dislocation and a screw dislocation. The edge component of the dislocation has an eight-atom ring structure, showing distortions in the *x-y* plane (as seen in the *Z*-contrast image), but no distortions in the *z* direction. In this image, the similarity in intensity between the core and the surrounding columns indicates that the composition is approximately unchanged (within ~10% accuracy), and the core can be considered intrinsic. Unlike the edge dislocation, the screw dislocation has a bulk hexagonal structure in the *x-y* plane and distortions solely in the *z* direction, as seen from the strain field in the image. The third type of dislocation is a mixed dislocation, which is a linear combination of the edge and screw cores. It has an eight-atom ring structure in the *x-y* plane, but also has a screw component in the *z* direction. It should be noted that in a *Z*-contrast image, the only differentiating factor between pure edge and mixed dislocations is the strain field, which is often very difficult to distinguish during the experiment. This factor will be discussed further in the following sections in relation to the electronic structures of mixed and edge dislocations.

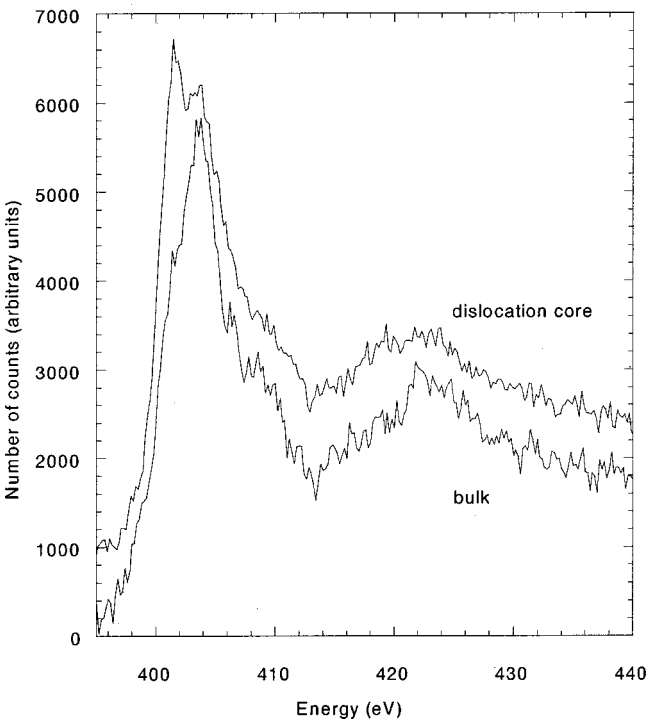

FIG. 2. Electron-energy-loss spectra (EELS) from the bulk and edge-component dislocation core. The core shows an increase of the unoccupied density of states above the conduction band onset with respect to the bulk. The core spectrum does not show a shift in the edge onset, implying that it is not intrinsically electrically active (Ref. 34). These spectra, as with all other figures in this paper, are shifted vertically for clarify.

Figure 2 shows nitrogen *K*-edge spectra obtained from bulk GaN and a dislocation core with edge character. Each spectrum is the sum of ten different spectra taken from three different edge-type dislocation cores with an acquisition time of 5 s each. Short acquisition times and multiple cores were used to avoid any possibility of beam-damage, induced artifacts in the spectra. Of particular interest is an increase in the unoccupied density of states at the conduction-band onset. However, it should be noted that there is no shift in the edge onset energy within the ~1-eV experimental energy resolution. Therefore, the experiment does not show any obvious states in the band gap, implying that there is no intrinsic electrical activity at these cores. It should also be noted that the changes in the spectral fine structure are extremely local to the dislocation core, with the bulk spectrum

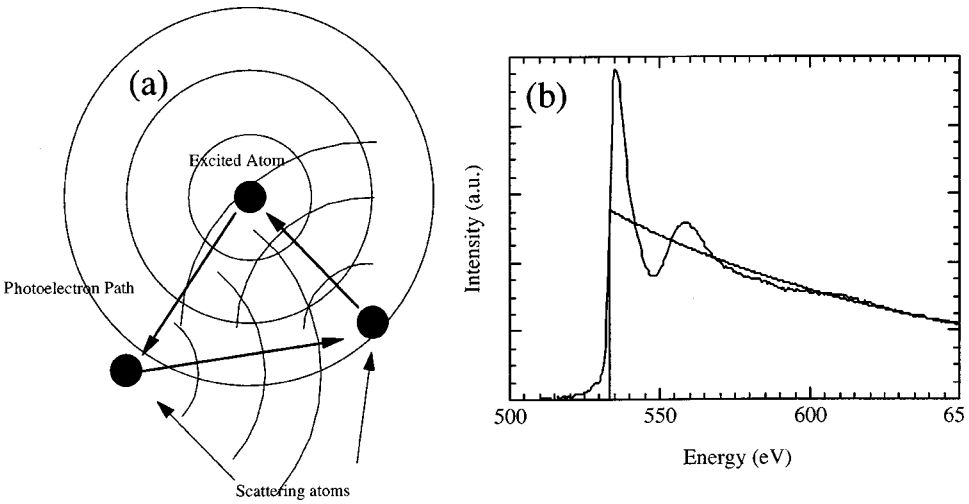

FIG. 3. Schematic of the multiple-scattering methodology. (a) The excited electron, in the form of a spherical wave, interacts with the surrounding atoms to form an interference pattern. (b) The interference effects modify the hydrogenic absorption edge expected for an isolated atom.

occurring only one unit cell away from the core.

III. DEFINING THE SIMULATION PARAMETERS

To understand the origin of the changes in the electronic structure occurring at dislocation cores (Fig. 2), we perform multiple scattering (MS) simulations using the FEFF8 codes.[22] FEFF8 is a set of programs implemented in an *ab initio* code that is based on a self-consistent real-space multiple-scattering (RSMS) theory for x-ray-absorption near-edge structure (XANES) calculations of periodic and aperiodic systems. The calculations make use of the single-particle Green's function, which is common to both XANES and electronic structure calculations. An advantage of this method for the analysis of dislocations is that calculations for large clusters may be attained in a relatively short time period because it uses full MS calculations to obtain the contribution to the Green's function from a small cluster of less than 100 atoms, and a high-order MS expansion for important paths that extend outside the cluster.

Another advantage of the MS approach is in its use of real-space clusters, and its ease in the interpretation of the resulting spectrum. In very basic terms, it is assumed that an excited photoelectron is emitted from the central atom in the cluster of interest as a spherical wave. This spherical wave is reflected during interaction with the surrounding atoms, and interferes with the outgoing wave, with the subsequent interference pattern mapping out the local density of unoccupied states (Fig. 3). This modeling technique has been applied in the past to x-ray absorption, and its application to electron absorption is exactly analogous; only the method of excitation has changed.[22–25] For an analysis of defect structures, the real-space clusters allow the dimensions and composition of the cluster to be constructed one atom at a time.[23] Therefore, the known lack of symmetry does not seriously affect the calculation, unlike more complex density-functional calculations.[38] Furthermore, the effects of vacancies and dopant atoms may be simply investigated by the removal or addition of the desired atoms. Hence the MS simulations allow the spectral changes (i.e., changes in the local electronic structure) to be interpreted directly in terms of the structural changes occurring at defects.

Before starting the MS analysis of defects, there are several key parameters that need to be determined for the specific material in question. The first and most important parameter is the radius for the self-consistent-field (SCF) calculations. The self-consistent-field approach in the FEFF8 codes is similar to other *ab initio* electronic structure calculations, in that it assumes that each electron moves independently in the average field of all the other electrons and the nuclei; this is calculated by density-functional theory.[38] The foundation of the self-consistency problem is the nonlinear dependence of the electron density on the potential, which in turn depends on the electron density through the electrostatic and exchange-correlation parts of the total energy and may only be determined using iteration techniques. The iterations for self-consistency are contained within the FEFF8 codes, with only the radius of the calculations to be determined by the user. We have found that the SCF radius must be at least the same as that of the cluster to ensure that the self-consistent energy calculations take all atoms into account. While the first few shells may have the largest impact on the SCF calculations, inclusion of all of the atoms yields a more accurate, though more time-consuming, calculation. This addition of self-consistency to the FEFF8 codes (which FEFF7 did not have) greatly reduces the inaccuracies and number of fitting parameters available to the user, that without care can lead to an unphysical or unrealistic match with the experimental data.[22,39]

The next key parameter to be identified for a series of simulations is the radius of convergence. This is done for all spectra presented here by increasing the cluster size for bulk GaN until there is no visible difference in the fine structure. This can also be done in FEFF8 by increasing or decreasing the full multiple scattering radius while keeping the number of shells constant. For GaN, and for most structures, convergence is achieved between six and seven shells (which means the clusters contain 50–120 atoms within a radius of $\sim$4.5–6 Å).[22] The simulations for shells 4–7 are shown in Fig. 4 to demonstrate the level convergence attained for bulk GaN. As the spectrum for seven shells is similar to that for six shells, it is assumed that convergence is reached at six shells and all subsequent simulations in this paper are per-

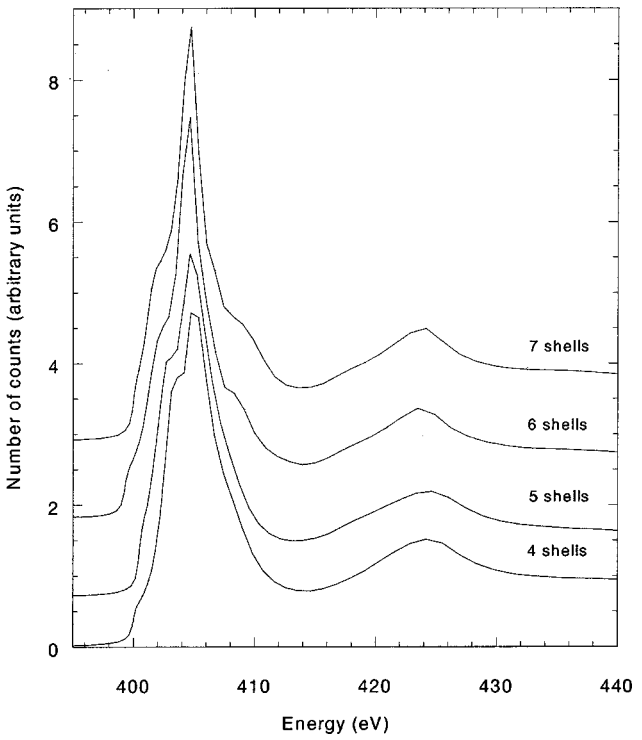

FIG. 4. Convergence for bulk GaN is found by simulating increasingly large clusters and observing when there are no further changes in fine structure. The spectrum for six shells is almost identical to that of seven shells; therefore, convergence is reached at six shells and all further simulations are run using clusters of this size.

formed for clusters of this size.

The final main user-defined functions in the simulations take into account the core hole and a broadening of the spectral features (which is set to 1 eV to match the experimental results shown above). It is well known that the experimental energy-loss spectra do not precisely match the unoccupied density of states. This is because the ejection of a 1*s* electron in the transition to the unoccupied states leaves behind a core hole which distorts the band structure. It is therefore important to include core hole effects in the simulations[40] of experimental energy-loss spectra, which is achieved in FEFF8 (and is included in all the calculations shown here) through the $Z+1$ approximation.[23,34]

For comparison with energy-loss spectra obtained from a microscope, the experimental acquisition conditions must be included. In the electron microscope, circular apertures are used to form the probe and collect the scattering in the spectrometer (Fig. 5). This means that the spectrum that is obtained contains electronic transitions from a range of incident and collection angles. In isotropic materials, the specimen orientation has no effect on the relative weighting of these electronic transitions. However, for anisotropic materials such as GaN, the fine structure of the spectra may be heavily dependent on the specimen orientation, since certain transitions may be preferentially selected in a given orientation (along the *c* axis or along the *ab* plane). Defects are certainly anisotropic areas of the specimen, and as such, it is important to determine the relative number of transitions for each component in order to perform an accurate analysis of the experimental spectra. Since the exact contribution from each component is dependent on the predetermined specimen orientation, probe convergence angle, and collection angle, the ratio of these transitions may be controlled and calculated. Previous studies of this effect show that the ratio of the transitions are calculated using this energy-loss function[41,42]

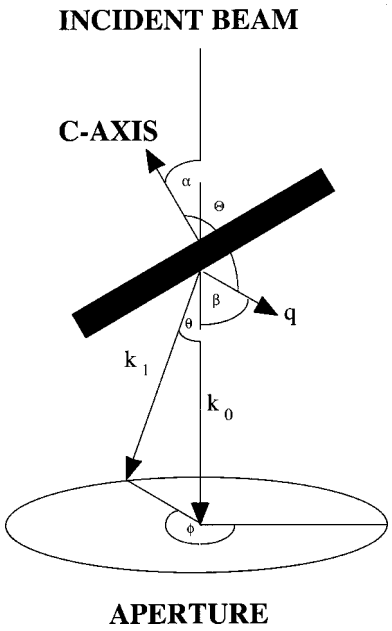

FIG. 5. Experimental acquisition conditions are taken into account when running the MS simulations to achieve a more accurate fit with the experimental spectrum. The parallel and perpendicular (to the *c* axis) components of the momentum transfer are dependent on the aperture size.

$$\mathcal{E}=(\varepsilon_2^{\perp}-\varepsilon_3'')\left(\frac{\theta_C^2}{\theta_C^2+\theta_E^2}\right)+(\varepsilon_2^{\perp}+\varepsilon'')\ln\left(1+\frac{\theta_C^2}{\theta_E^2}\right) \qquad (1)$$

where θ_C is the collection angle, θ_E is the characteristic angle[43] for a given energy loss ($\theta_E=\Delta E/2E$, where E is the beam energy and ΔE is the energy loss) and $\varepsilon_2^{\perp}$ and ε_2'' are the perpendicular and parallel components of the imaginary parts of the dielectric function. For the experimental conditions in the JEOL 2010-F, this ratio was calculated to be 43% for the parallel components and 57% for the perpendicular component for an aperture size of 38 mrad with the specimen in the (0001) orientation. In the MS analysis shown here, the overall spectrum is obtained by running two simulations for each cluster polarized in the *c* and *ab* directions, and then multiplying these simulations by the ratio given above.

IV. MULTIPLE SCATTERING SIMULATIONS

A. Bulk

The first step in the analysis of dislocations in GaN is to simulate the bulk structure to ensure that the few user-defined parameters are realistic. Additionally, as the atom positions have already been accurately determined by x-ray diffraction, this simulation requires the least input data. This

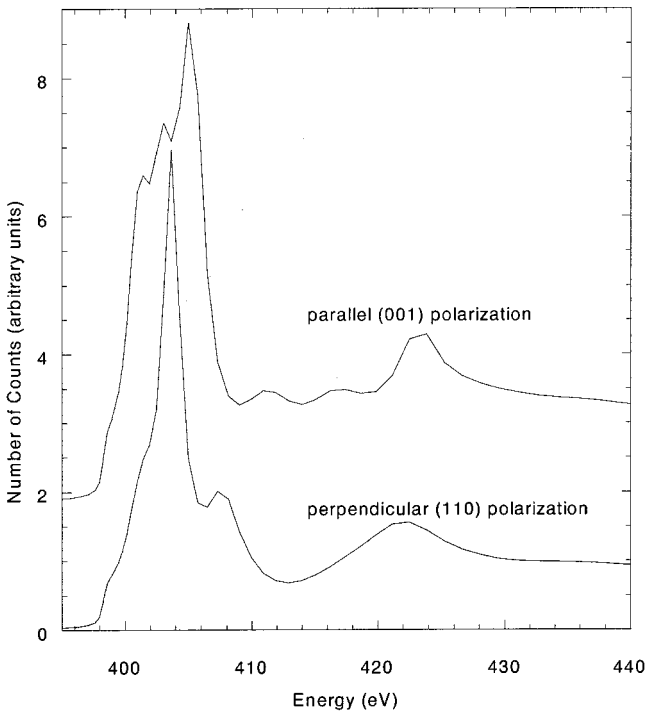

FIG. 6. The fully parallel and perpendicularly polarized components of bulk GaN.

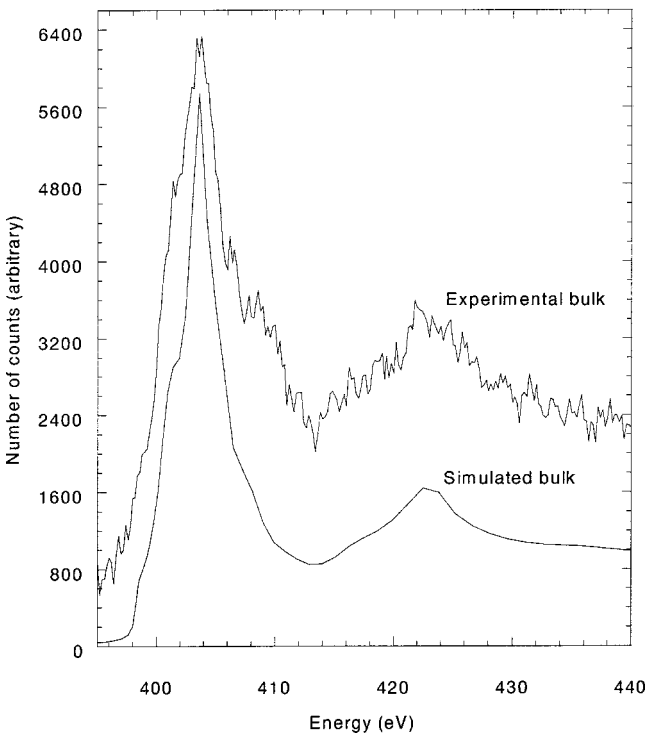

FIG. 7. The MS simulation of the bulk is in good agreement with the experimental spectrum, demonstrating the accuracy of the parameters used.

means that parameters that are determined for the bulk can then be used for all of the dislocation core simulations. Following the procedure discussed above, the perpendicular and parallel components of the bulk are simulated separately (Fig. 6), and then added together with relative weighting for each component. Figure 7 is a comparison of the simulated bulk spectrum with the experimental spectrum. It shows that the fine structure is accurately reproduced, with only slight differences in intensity at higher-energy losses due to plural scattering effects in the experimental spectra.[43] These spectra are also identical to those obtained from XANES studies,[44] supporting the accuracy of the parameters, potentials, and cluster sizes used for these simulations.

B. Dislocation cores

With the simulation parameters in place, the more complex dislocation cores may now be investigated. The dislocation with the least amount of distortions and most abundant in the GaN thin-film material used in this experimental study is the edge dislocation.[34] From the definition of an edge dislocation[2] distortions exist only in the *x*-*y* plane, and the atomic spacing is bulklike in the *z*-direction. As *z*-contrast images (Fig. 1) are incoherent, coordinates for the atom locations may be taken directly from them. Assuming that the columns maintain their bulklike separation along the *c* axis, this permits clusters to be constructed for the MS simulations directly from the experimental data. However, before putting these clusters into the MS program, we can improve the accuracy of the simulations by using distance-valence least squares (DVLS) analysis.[27–30] DVLS analysis is an important first step, as it helps to reduce the errors in the inaccuracies of the positions of the atoms caused by the *Z*-contrast technique.[45] Although these errors are typically only ~0.2 Å, and are caused by the fact that the STEM is very sensitive to electrical, thermal, and mechanical instabilities, they can affect the simulations.

The DVLS analysis assumes that the formal valence-state of each atom is a sum of the contributions from all the nearest neighbors, and that these contributions should be shared equally between all the nearest neighbors. Using the atom coordinates from the image, a simple minimization of the differences from the expected valences and bond lengths can be performed using the relation

$$S = \exp\left(\frac{r_{ij} - r_0}{B}\right) \tag{2}$$

where r_{ij} is the bond length between atoms i and j, r_0 is the equilibrium bond length, and B is an empirically determined constant ($B = 0.37$).[27,28] This simple pair potential between two atoms is used to calculate the valences and bond lengths in the structure to check if the positions of the atoms are reasonable. It will produce a high valence if the bond length between any two atoms is too short, or a low valence if the bond length is too long. By shifting the atoms (a maximum of ~0.2 Å) to achieve the best valences, the program effectively runs an energy minimization. While this minimization cannot compare in accuracy to that of *ab initio* calculations, it can verify that a physically reasonable structure exists (within 10% error) in a minimal amount of time.[45] The DVLS (also called bond-valence) analysis for the edge, screw, and mixed dislocations in this paper was performed

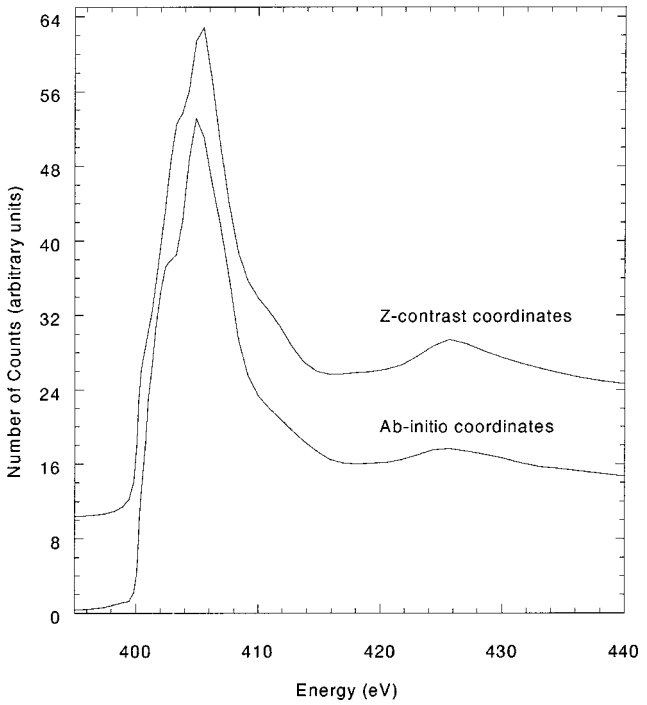

FIG. 8. MS simulations for the edge dislocation using the *Z*-contrast method and using *ab initio* calculated coordinates. The spectra are almost identical suggesting that the atomic coordinates derived from the *Z*-contrast image are essentially the same as those calculated from first principles.

using cell sizes of 2–3 unit cells around the core and 2–5 unit cells thick (the smaller cells are used for the edge dislocation whereas the larger ones are used for the mixed and screw dislocations), including approximately 130–380 atoms. In all cases the structures resulted in atoms with valences close to the expected formal valence states of ± 3 for Ga and N. Having verified that the core structures were consistent with the chemistry of the elements involved, the clusters were constructed for MS analysis.

Edge dislocation

As dislocations break the symmetry of the bulk structure,[2] all sites of the core must be taken as distinct sites and simulated separately. An assumption of symmetry in any direction at a dislocation core does not yield an accurate result on the atomic scale, because a difference of even a small fraction of an Å will result in a different and incorrect interference pattern from the MS calculations. However, although the spatial resolution of the experimental spectrum is potentially 0.13 nm (i.e., the probe size), which allows individual sites to be observed, instabilities tend to broaden the information that is obtained to the core as a whole. As such, a comparison of the simulations to the experimental spectrum must contain the sum of all the individual sites. The resulting simulation for the edge dislocation, including all eight distinct sites at the core and taking into account the collection conditions, is shown in Fig. 8. Also shown in Fig. 8 is the MS simulation performed in the same way, but building the clusters from the *ab initio* calculated coordinates.[18,19] The two calculations are remarkably similar, suggesting that the atomic coordinates derived from the *Z*-contrast image are essentially the same as those calculated from first principles.

Screw dislocation

In the screw dislocation, the distortions are all in the *c* direction with the bulk hexagonal structure being observed in the *x*-*y* plane (Fig. 1). Thus the method described to build the edge dislocation cannot be applied to this particular defect (there is no change in the bulk structure observed in the image). To overcome this problem, linear elasticity theory[1,2] was used to calculate the positions of the atoms within the constraint of the hexagonal structure observed in the image. For this theory to be used, the stresses and strains that arise from the displacement of atoms from their bulk lattice sites must be very small. We see this must be the case for our analysis, as the periodicity of the columns in the *x*-*y* plane is still present in the *Z*-contrast image (if the distortions were too large, they would shift the atoms out of the columns). While it is thought that linear elasticity breaks down at distances close to dislocation cores, this is not a major problem for the analysis here since the DVLS minimization corrects any inaccuracies in the atom positions. For the screw dislocation, the atom positions in and around the core can therefore be calculated from the simple relation[1,2]

$$D = -\left(\frac{b}{2\pi}\right)\arctan\left(\frac{y}{x}\right) \tag{3}$$

where D is the displacement in the z direction, b is the Burgers vector ($b=[000c]=5.19$ Å for GaN), and x and y refer to the *x*-*y* coordinates. By arbitrarily choosing a starting point on a geometrically created hexagonal structure (in the *x*-*y* plane), this equation can be used to calculate the distortions in the *c* direction column by column. After constructing the core in this manner and minimizing the atom positions using the DVLS calculations, clusters were constructed for all six distinct sites around the screw dislocation. The MS simulation obtained after the summation of all of these sites is shown in Fig. 9. As it is not possible to image the distortions in the *c* direction in the screw dislocation, *ab initio* calculated coordinates[18,19] were used to verify the results from linear elasticity. Figure 9 also shows the simulation from the *ab initio* coordinates, illustrating the similarities in both the intensities and energies of the fine structure peaks in the spectrum.

Mixed dislocation

As with the screw dislocation, it is not possible to obtain a direct image of the atom positions in the mixed core. However, as the mixed dislocation contains a combination of the screw and edge components of the Burgers vector, clusters for multiple-scattering simulations can be calculated from the previous analyses. In this regard, *ab initio* coordinates were used for the edge component, and linear elasticity was used to add the screw component, with a bond-valence analysis used to minimize the atom positions in the structure (given the results from the edge and screw simulations, this approach seems justified). Figure 10 shows the results of the

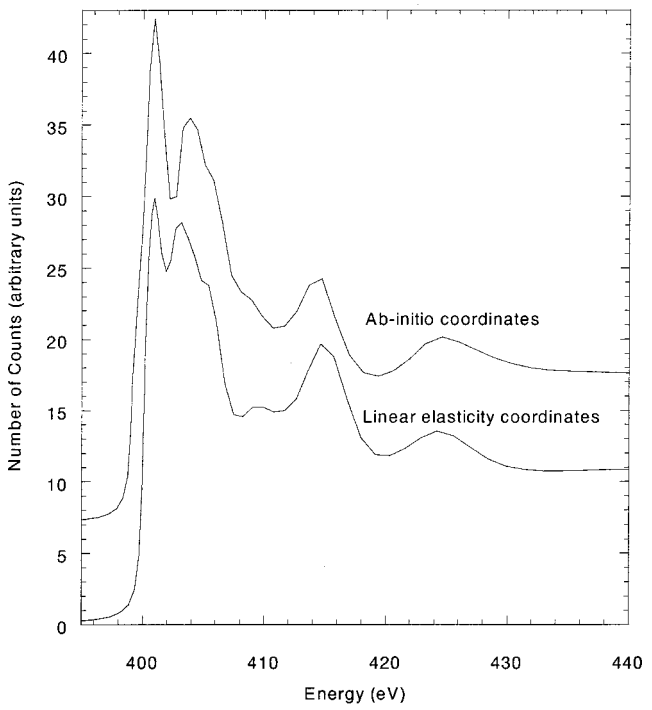

FIG. 9. MS simulation of the screw dislocation using the linear elasticity method and using *ab initio* calculated coordinates. Once again, we see strong similarities in the energies and intensities of the spectra, suggesting that the atomic coordinates are similar using both methods.

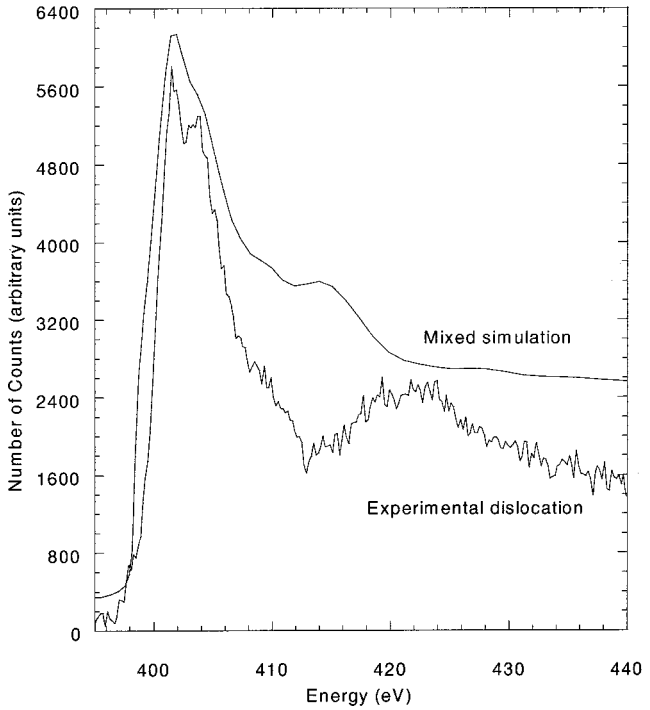

FIG. 10. MS simulation of the mixed dislocation and the experimental edge character dislocation. Not obvious from the *Z*-contrast image of Fig. 1, the dislocation is in fact of mixed type rather than pure edge, seen from the similarities of the electronic structures shown here. Small changes in fine structure are attributed to experimental discrepancies.

MS simulation (with the eight distinct sites included) for the constructed core. As full *ab initio* calculations have not been performed for the mixed dislocation core, there is no independent verification of the result possible. For comparison purposes, the experimental result from the dislocation core is also plotted in Fig. 10.

V. DISCUSSION

As can be seen from Fig. 7, the self-consistent MS simulation accurately reproduces the experimental nitrogen *K*-edge spectrum for bulk GaN. This good agreement between the simulation and experiment provides confidence in the ability of these routines to simulate the electronic structure at the dislocation cores. However, the MS simulation of the edge dislocation (Fig. 8) does not match the experimental spectrum of the dislocation with an edge component (Fig. 2) at all, suggesting that the dislocation analyzed experimentally may have been of mixed nature (for which the only difference in the image is the intensity variations caused by the strain field). This hypothesis is supprted by the fact that the spectra obtained using atom positions from the *ab initio* calculations and the *Z*-contrast images are virtually identifcal for the edge and screw dislocations. The electronic structure of the mixed dislocation shown in Fig. 10 is in fact very similar to that of the experimental spectrum from the dislocation with the edge component. The first two peaks are almost identical, with an increase in intensity in the third peak (at 415 eV) of the mixed dislocation simulation being attributed to the contribution of the screw component (Fig. 9). It should be noted that the linear elasticity plus DVLS simulations of the screw dislocation overestimate the intensity of this peak (Fig. 8), and this is carried through to the simulation from the mixed dislocation.

The lack of this feature at 415 eV in the experimental spectrum suggests that the contributions to the experimental spectrum might be two thirds from a mixed dislocation and one third from an edge dislocation, or vice versa (since the experiment was performed from three separate cores). However, upon further analysis, it was found that adding the mixed dislocation to the edge dislocation in these proportions does *not* yield the experimental spectrum (the statistics of the individual spectra also preclude an analysis of the individual acquisitions). An alternative explanation for the slight differences between the experimental spectrum and the MS spectrum for the mixed dislocation core is experimental errors. These discrepancies could arise from errors in the atomic positions due to instability in the microscope or by drift of the specimen during acquisition of the spectrum. Of these, the second reason seems most likely.[34] As found during the experiment, movement of only a single unit cell away from the dislocation core resulted in a spectrum that was more bulklike. This means that any small shift or drift in the experiment could cause an increase in one of the peaks. Unless the probe is placed directly on top of the central atomic site in the dislocation, which is again hard to maintain because of drift, small variations in the fine structure between the experiment and the simulation are entirely possible due to the nature of the experimental limitations.

A comparison of the simulations from all three disloca-

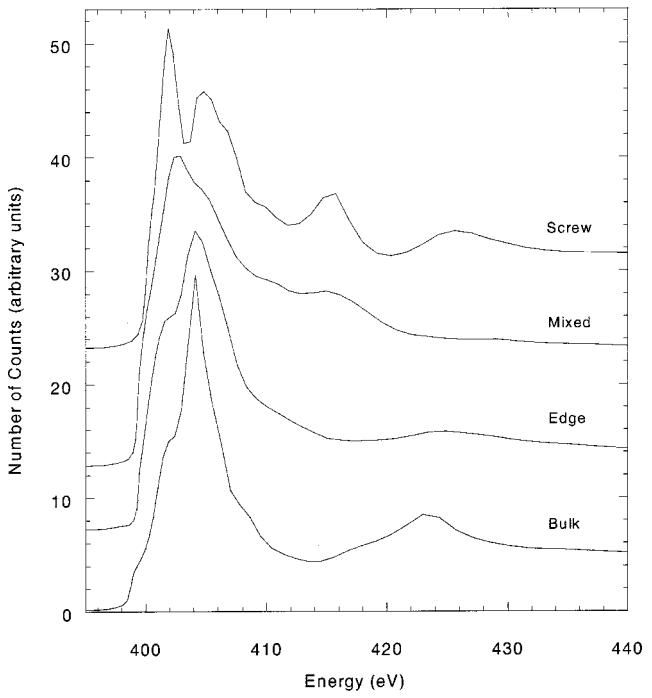

FIG. 11. Bulk GaN is plotted with the three dislocation cores of GaN. The edge dislocation is almost bulklike, due to its small distortions and bulklike nearest neighbors. The distortions in the *c* direction present in both the screw and mixed dislocations produce a strong first peak above the conduction-band onset. The edge component of the mixed dislocation acts to broaden some of its features, but the ratios of the peaks intensitites are still maintained.

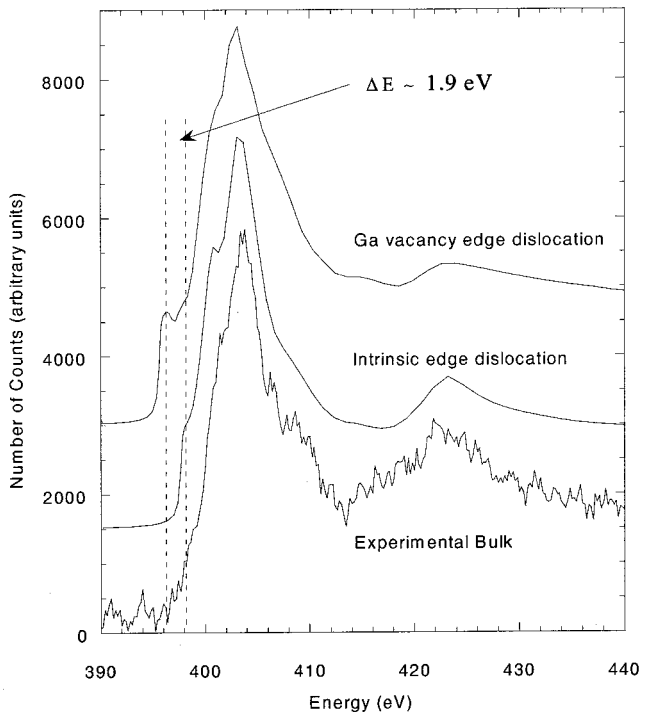

FIG. 12. Simulation from an edge dislocation containing Ga vacancies, plotted with the intrinsic edge dislocation and the experimental bulk. The dotted line at ~398 eV shows the same peaks appearing in the bulk and intrinsic edge dislocation, while the line at ~396 eV shows a peak at ~1.9 eV below the edge onset for the edge dislocation with Ga vacancies, suggesting the possible creation of a state in the band gap.

tions and the bulk is shown in Fig. 11. The spectrum from the edge dislocation appears to be almost bulklike. Examination of the clusters suggests that this should be expected, since the nearest neighbors for most of the core atom positions are very close to bulklike nearest neighbors (and there is only a small strain field in the *a*-*b* plane). The major changes in the fine structure of the dislocation cores appears to arise from the presence of the screw component to the Burgers vector. As can be seen from the simulation of the mixed dislocation core, the addition of the screw component increases the intensity in the peak just above the edge onset. This peak is further enhanced in the simulation from the screw dislocation. Furthermore, the presence of the screw component also leads to a peak at 415 eV that is not present in either the bulk or edge dislocation.

Despite these changes in the fine structure, all of the dislocation cores are consistent in not showing the presence of localized states in the band gap. The edge onsets from all of the simulations are within ~1 eV of each other, and are consistent with the experimental edges (a shift of ~1 eV was required). If the intrinsic dislocation cores were electrically active, changes in the position of the onset would be expected to be more significant. It should be noted that the accuracy in the positioning of the edge onset is only expected to be ~1 eV. This means that changes in activity may be difficult to observe in the simulations. However, the fact that the simulations are consistent with the experiment indicates that the lack of intrinsic activity observed in the cores is a real effect.

This lack of activity is consistent with studies of grain boundaries in oxides,[35] where it was found that the dislocation core structure in the boundary did not significantly change the band gap or lead to localized states in the band gap. However, in this case the structure of the boundary did create a segregation energy for vacancies in the structure that led to local activity at the boundary plane.

Similar conclusions for dislocations in GaN are supported by preliminary simulations for an edge dislocation containing Ga vacancies (Fig. 12). Here all of the Ga atoms were removed from the central column in the dislocation core, consistent with previous theoretical models.[15] The structures were subsequently allowed to relax through the DVLS analysis and the clusters constructed as with the previous analysis. As can be seen from Fig. 12, the presence of Ga vacancies in the dislocation core leads to the formation of a peak ~1.9 eV below the edge onset, i.e., localized states are formed in the band gap. Future work will examine the effect of Ga vacancies at the other dislocations, as well as the effect of N vacancies on the local density of unoccupied states.

VI. CONCLUSIONS

Self-consistent multiple-scattering simulations of the nitrogen *K*-edge spectra from the bulk, edge, screw, and

mixed dislocations in GaN have been performed. The simulation of the bulk spectrum shows excellent agreement with the experiment and indicates the ability of the FEFF8 codes to generate accurate results. The simulations of the nitrogen *K* edges from the dislocation cores indicate that the experimental spectrum obtained from a core with an edge character to the Burgers vector to be consistent with a mixed dislocation. All of the experimental and theoretical spectra are consistent with there being no states in the band gap for these intrinsic cores. This indicates that device performance is more likely limited by impurities and the segregation of vacancies to the cores over time. This effect may explain the differences in the experimental results obtained by different groups. Future experimental and theoretical work will focus on examining the effects of vacancies and impurities at dislocations in GaN.

ACKNOWLEDGMENTS

We would like to thank Y. Xin, E. M. James, S. J. Pennycook, F. Omnes, B. Beaumont, J. P. Faurie, and P. Gibart for the experimental results, and we are grateful to A. Blumenau and J. Elsner for the *ab initio* coordinates used in these simulations. This research was supported by the National Science Foundation under Grant No. DMR-9733895, and in part by the Materials Research Society by an undergraduate materials research initiative (UMRI) award.

[1] J. P. Hirth and J. Lothe, *Theory of Dislocations*, (Wiley, New York, 1982).
[2] D. Hull and D. J. Bacon, *Introduction to Dislocations*, 3rd ed. (Pergamon, New York, 1997).
[3] K. Kusakabe, K. Kishino, A. Kikuchi, T. Yamada, D. Sugihara, and S. Nakamura, J. Crys. Growth **230**, 387 (2001).
[4] S. Nakamura, M. Senoh, S. Nagahama, N. Iwasa, T. Yamada, T. Matsushita, H. Kiyoku, Y. Sugimoto, T. Kozaki, H. Umemoto, M. Sano, and K. Chocho, Jpn. J. Appl. Phys., Part 2 **37**, L309 (1998).
[5] S. Nakamura, Science **281**, 956 (1998).
[6] S. D. Lester, F. A. Ponce, M. G. Craford, and D. A. Steigerwald, Appl. Phys. Lett. **66**, 1249 (1995).
[7] P. Vennegues, B. Beaumont, V. Bousquet, M. Vaille, and P. Gibart, J. Appl. Phys. **87**, 4175 (2000).
[8] S. M. Nilsen, H. Gronqvist, H. Hjelmgren, A. Rydberg, and E. L. Kollberg, IEEE Trans. Microwave Theory Tech. **41**, 572 (1993).
[9] S. J. Rosner, E. C. Carr, M. J. Ludowise, G. Girolami, and H. I. Erikson, Appl. Phys. Lett. **70**, 420 (1997).
[10] M. Hao, S. Mahanty, T. Sugahara, Y. Morishima, H. Takenaka, J. Wang, S. Tottori, K. Nishino, Y. Naoi, and S. Sakai, J. Appl. Phys. **85**, 6497 (1999).
[11] S. Dassonneville, A. Amokrane, B. Sieber, J.-L. Farvacque, B. Beaumont, and P. Gibart, J. Appl. Phys. **89**, 3736 (2001).
[12] T. Izumi, Y. Narukawa, K. Okamoto, Y. Kawakami, Sg. Fujita, and S. Nakamura, J. Lumin. **87–89**, 1196 (2000).
[13] C. Youtsey, L. T. Romano, R. J. Molnar, and I. Adesida, Appl. Phys. Lett. **74**, 3537 (1999).
[14] N. G. Weimann, L. F. Eastman, D. Doppalapudi, H. M. Ng, and T. D. Moustakas, J. Appl. Phys. **83**, 3656 (1998).
[15] D. C. Look and J. R. Sizelove, Phys. Rev. Lett. **82**, 1237 (1999).
[16] P. J. Hansen, Y. E. Strausser, A. N. Erickson, E. J. Tarsa, P. Kozodoy, E. G. Brazel, J. P. Ibbetson, U. Mishra, V. Narayanamurti, S. P. DenBaars, and J. S. Speck, Appl. Phys. Lett. **72**, 2247 (1998).
[17] K. V. Smith, E. T. Yu, J. M. Redwing, and K. S. Boutros, J. Electron. Mater. **29**, 274 (2000).
[18] J. Elsner, R. Jones, P. K. Sitch, V. D. Porezag, M. Elstner, Th. Frauenheim, M. I. Heggie, S. Öberg, and P. R. Briddon, Phys. Rev. Lett. **79**, 3672 (1997).
[19] J. Elsner, R. Jones, M. I. Heggie, P. K. Sitch, M. Haugk, Th. Frauenheim, S. Öberg, and P. R. Briddon, Phys. Rev. B **58**, 12 571 (1998).
[20] A. F. Wright and U. Grossner, Appl. Phys. Lett. **73**, 2751 (1998).
[21] R. Jones, Mater. Sci. Eng., B **71**, 24 (2000).
[22] A. L. Ankudinov, B. Ravel, J. J. Rehr, and S. D. Conradson, Phys. Rev. B **58**, 7565 (1998).
[23] Andrew J. Scott, Rik Brydson, Maureen MacKenzie, and Alan J. Craven, Phys. Rev. B **63**, 245 105 (2001).
[24] N. D. Browning, H. O. Moltaji, and J. P. Buban, Phys. Rev. B **58**, 8289 (1998).
[25] M. K. H. Natusch, G. A. Botton, C. J. Humphreys, and O. L. Krivanek, IOP Conf. Proc. No. 153 (Institute of Physics and Physical Society, Bristol, 1997), p. 339.
[26] S. J. Pennycook and L. A. Boatner, Nature (London) **336**, 565 (1988).
[27] D. Altermatt and I. D. Brown, Acta Crystallogr., Sect. B: Struct. Sci. **41**, 240 (1985).
[28] I. D. Brown and D. Altermatt, Acta Crystallogr., Sect. B: Struct. Sci. **41**, 244 (1985).
[29] N. D. Browning and S. J. Pennycook, J. Phys. D **29**, 1779 (1996).
[30] N. D. Browning, J. P. Buban, H. O. Moltaji, and G. Duscher, J. Am. Ceram. Soc. **82**, 366 (1999).
[31] S. J. Pennycook and D. E. Jesson, Phys. Rev. Lett. **64**, 938 (1990).
[32] P. D. Nellist and S. J. Pennycook, Ultramicroscopy **78**, 111 (1999).
[33] Y. Xin, S. J. Pennycook, N. D. Browning, P. D. Nellist, S. Sivananthan, F. Omnes, B. Beaumont, J. P. Faurie, and P. Gibart, Appl. Phys. Lett. **72**, 2680 (1998).
[34] Y. Xin, E. M. James, I. Arslan, S. Sivananthan, N. D. Browning, S. J. Pennycook, F. Omnes, B. Beaumont, J. P. Faurie, and P. Gibart, Appl. Phys. Lett. **76**, 466 (2000).
[35] M. Kim, G. Duscher, N. D. Browning, K. Sohlberg, S. T. Pantelides, and S. J. Pennycook, Phys. Rev. Lett. **86**, 4056 (2001).
[36] P. D. Nellist and S. J. Pennycook, Adv. Imaging Electron Phys. **113**, 147 (2000).
[37] E. M. James and N. D. Browning, Ultramicroscopy **78**, 125 (1999).
[38] R. M. Dreizler and E. K. U. Gross, *Density Functional Theory: An Approach to the Quantum Many-Body Problem* (Springer-Verlag, Berlin, 1990).

[39] D. J. Wallis and N. D. Browning, J. Am. Ceram. Soc. **80**, 781 (1997).
[40] G. Duscher, R. Buczko, S. J. Pennycook, and S. T. Pantelides, Ultramicroscopy **86**, 355 (2001).
[41] N. D. Browning, J. Yuan, and L. M. Brown, Ultramicroscopy **38**, 291 (1991).
[42] N. D. Browning, J. Yuan, and L. M. Brown, Philos. Mag. A **67**, 261 (1993).
[43] R. F. Egerton, *Electron Energy-Loss Spectroscopy in the Electron Microscope*, 2nd ed. (Plenum, New York, 1996).
[44] M. Katsikini, E. C. Paloura, and T. D. Moustakas, J. Appl. Phys. **83**, 1437 (1998).
[45] N. D. Browning, J. P. Buban, P. D. Nellist, D. P. Norton, and S. J. Pennycook, Physica C **294**, 183 (1998).